Fizika Nizkikh Temperatur, 1999, v. 25, No 10, p.1082–1086

Proximity phenomena in double-barrier structure $NbZr / NbO_x / Al / AlO_y / NbZr$

A. Plecenik, Š. Gaži, M. Zuzčak, and Š. Beňačka

Institute of Electrical Engineering, Slovak Academy of Sciences,Dubravska cesta 9, 84239 Bratislava, Slovak Republic
E-mail: plecenik@savba.sk

V. Shaternik and E. Rudenko

Institute for Metal Physics, National Academy of Sciences of Ukraine, 36 Vernadsky Str., 252142 Kiev, Ukraine
E-mail: shat@d24.imp.kiev.ua

Received February 1, 1999, revised March 19, 1999

A tunneling structures $NbZr/NbO_x/Al/AlO_y/NbZr$ with a thin barrier in the $NbZr/NbO_x/Al$ junction and 4 to 6-nm-thick Al interlayer were prepared and studied experimentally. A proximity effect between NbZr and Al through NbO_x barrier has been observed. An electrical voltage was generated in the NbO_x barrier and a coexistence of the proximity effect and applied voltage in the junction $NbZr/NbO_x/Al$ has been observed. This experiment could be described on the basis of a model for coherent charge transport in superconducting/normal proximity structures.

PACS: 74.80.Fp

1. Introduction

Tunneling process permits to obtain information on the superconducting density of states (DOS) over a wide energy range with high-energy resolution, both for superconductors in the equilibrium state and for those in the nonequilibrium state. The proximity effect between a superconductor and normal metal has been discussed for a long time, and it has recently attracted new attention because of the dramatic progress in nanotechnology, which allows the fabrication and study of tunneling structures in the mesoscopic regime [1]. The electron transport in normal diffusive conductors in the presence of proximity-induced superconducting correlation was studied theoretically in Ref. 2. It was demonstrated in Ref. 2, in the case of transparent barriers, superconducting correlations and electrical field can penetrate, causing a whole range of novel effects. In this paper we report on the observation of the coexistence of proximity-induced superconducting correlation and electrical field.

2. Experimental

Superconducting thin films were deposited by dc magnetron sputtering from Nb target with admixture of Zr, and clean target of Al. After the deposition of 100 nm thick NbZr film ($T_c \approx 12$ K) the first tunneling barrier (NbO_x) was prepared in two technological steps. At first, the thermal oxidation of NbZr in O_2 at room temperature was provided and then the tunneling barrier was finished by rf sputter-oxidation in Ar and residual gas. In this step thin, dirty NbZr layer, implanted by O_2 at energies 250–500 eV, was prepared. Specific contact resistance R of this junction is smaller in order than that of the top tunnel junction ($Al/AlO_y/NbZr$) resistance. After this procedure thin Al layer was deposited by dc sputtering at a deposition rate of 100 nm/min at 2 Pa of Ar. Then the thermal oxidation of Al was carried out at room temperature at 100 Pa for 60 min. After pumping of the vacuum system, the top layer of NbZr was deposited at 2 Pa with the deposition rate 160 nm/min. The top layer was deposited on a cooled substrate holder at about 10°C.

This technology provides nonsymmetrical operation of the double-barrier tunnel structure. The $I–V$

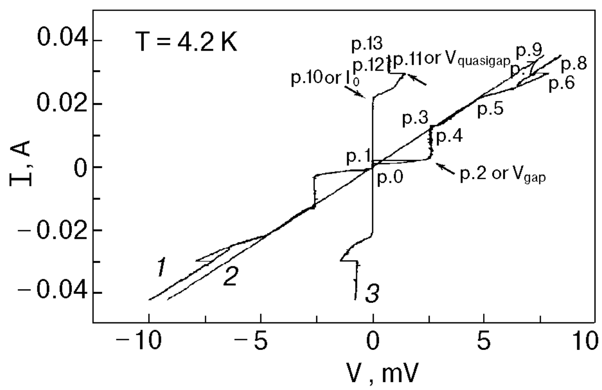

Fig. 1. The $I-V$ curves of the double-barrier structure NbZr/NbO_x/Al/AlO_y/NbZr .

characteristics of the structure are shown in Figs. 1–3 for various temperatures.

3. Discussion

We have investigated a superconducting tunnel junction with NbO_x and AlO_y potential barriers. One can see in Fig. 1 (curve *1*) the presence of a Josephson current (the $I-V$ curve from point p.0 to p.1) that flows through the double barriers. The NbO_x barrier resistance R is smaller in order than that of the AlO_y barrier. It is assumed that the AlO_y barrier limits the Josephson critical current through the double-barrier junction, but for the NbO_x barrier the Josephson critical current must be higher than that for the AlO_y barrier. In the experiment the same current flows through both barriers simultaneously; therefore at small current (to point 5) a voltage in the NbO_x barrier does not exist. One can see from point 1 to point 5 that the measured $I-V$ curve is a characteristic of a superconducting tunnel junction. For example, the proximity model [3,4] of NbZr/NbO_x/Pb and of

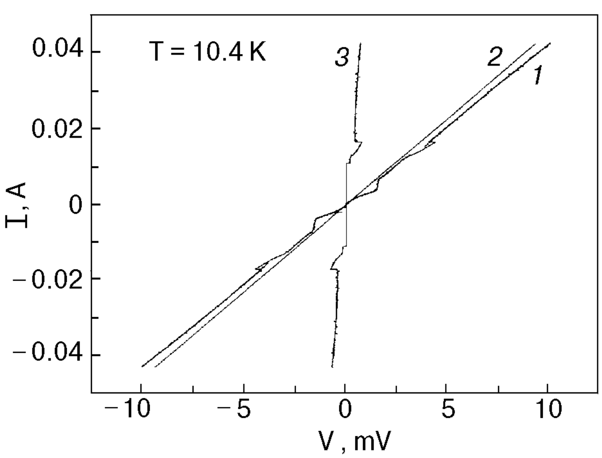

Fig. 2. The $I-V$ curves of the double-barrier structure NbZr/NbO_x/Al/AlO_y/NbZr .

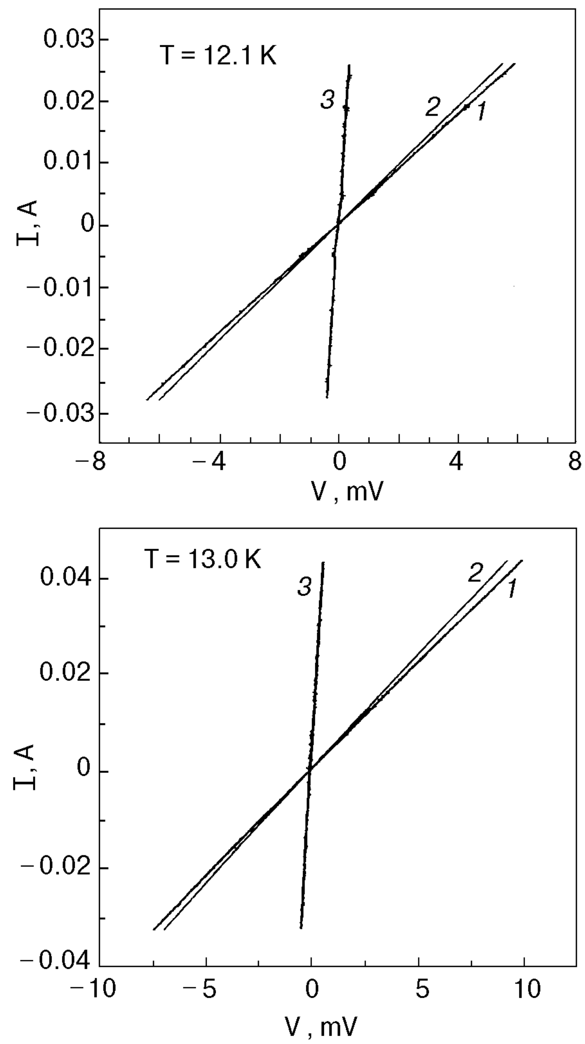

Fig. 3. The $I-V$ curves of the double-barrier structure NbZr/NbO_x/Al/AlO_y/NbZr .

NbN/NbO_x/Pb tunnel junctions, fabricated using similar technology, with the exception of thermal oxidation instead of rf-oxidation, shows good agreement between the calculated and experimentally determined values of the proximity layer. Now we can measure the current step on the junction (for example, point 2 or point 3 on the $I-V$ curve) and estimate the value of the proximity energy gap of Al. We conclude that the Al proximity energy gap value is approximately equal to $\Delta_{\rm Al}^{\rm Pr} \approx 1.2-1.3$ meV at $T = 4.2$ K.

The nature of this gap is in the proximity effect between the NbZr and Al through the NbO_x barrier. Also in the experiment the $\Delta_{\rm Al}^{\rm Pr}$ values change slightly because the Al film has a nonequilibrium quasiparticle distribution function induced by the current through the AlO_y barrier .

One can see $I-V$ curve is linear from point 4 to point 5. This part of the $I-V$ curve can be fitted by a linear function like $I = 4.6\ V$; this fitted curve is shown as curve *2*. At point 5, there is voltage also on the NbO_x barrier. At this point the current attains values of the critical current for the NbO_x barrier. Let us now analyze the $I-V$ curve as the «sum» of the two $I-V$ curves for the two junctions, because from this point the measured voltage is the sum of the voltage on the AlO_y barrier and the voltage on the NbO_x barrier. Voltage on the AlO_y barrier can be calculated by using the fitted curve *2* and corresponding value of the current through the junctions, $V_{AlO_y} = I/4.6$. We then calculate the voltage on the NbO_x barrier as $V_{NbO_x} = V - V_{AlO_y}$ and we plot the graph of the $I-V$ curve for the $NbZr/NbO_x/Al$ junction using the corresponding values of I and V_{NbO_x} (see curve *3* in Figs. 1–3).

We see that above point 5 there is voltage on the NbO_x barrier, and simultaneously the nature of the Al-«gap» is the proximity effect between NbZr and Al through the same NbO_x barrier. Proposed model could be analyzed on the basis of the new theory for coherent charge transport in superconducting/normal proximity structures [2].

The $I-V$ curves were measured in the range of temperatures T from 4.2 to 13 K (see Figs. 1–3). Since at $T > T_c^{NbZr}$ the $I-V$ curve is linear (see Fig. 3), NbZr and Al are in the normal state, and the large voltage does not exist on the NbO_x barrier. In the case $T > T_c^{NbZr}$ the voltage on the normal Al and NbO_x barrier is negligible.

Recall that unusual quasi-superconducting state exists in Al; we will compare the measured $I-V$ curves with the $I-V$ curves of the superconducting Josephson junctions. The constriction model for SNS Josephson junctions is well known. In this model the approach developed by Blonder, Tinkham, and Klapwijk (BTK) for calculation of the quasiparticle (qp) current in NcS contacts is generalized to the case of ScNS and SNcNS contacts with disordered NS electrodes. The relation between the qp current and the energy spectrum of NS proximity sandwich is found for arbitrary transparencies of the constriction and NS interfaces. We have plotted, for $NbZr/NbO_x/Al$ junction, the dependence of the critical current (point 10 on curve *3* in Figs. 1–3) on the temperature (see Fig. 4). Our curve likes the curve *2* in Fig. 2 (Ref. 5), it is a case for ScNS or SNcNS with $d_N/\xi_N = 1$, $\gamma_B = 1$, and $\gamma = 0$ ($\gamma_B = R_B/\rho_n\xi_n$, $\gamma = \rho_s\xi_s/\rho_n\xi_n$; here γ is a measure of the strength of the proximity effect between the S and N metals, and γ_B describes the effect of the boundary transparency between these layers; $\rho_{n,s}$ and $\xi_{n,s}$ are the normal state resistivities and coherence lengths, and R_B is the product of the resistance of the NS boundary and its area [5]). We can therefore assume that the Nb/Al interface is a series of constrictions in otherwise with lower transparent barriers.

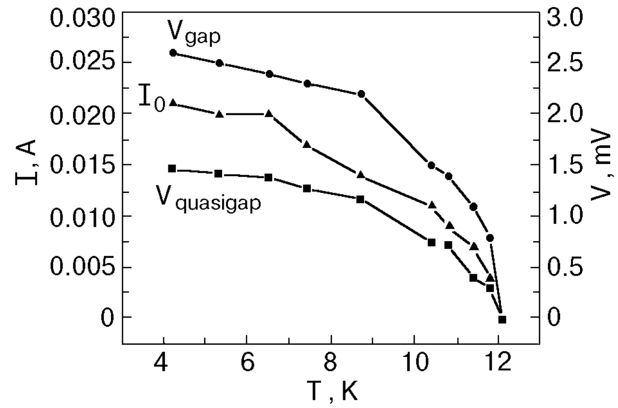

Fig. 4. The dependences of the critical current I_0, V_{gap}, $V_{quasigap}$ on temperature.

From point 10 to point 13 the $I-V$ curve is like an $I-V$ curve for a Josephson tunnel junction. With such shape the $I-V$ curves are described in Ref. 6 for the stacked Josephson tunnel junctions $Nb/Al-AlO_y/Nb$ of overlap geometry. This kind of $I-V$ curve can exist if the Al is in a quasi-superconducting state, but it cannot exist in the other cases.

We have plotted, for the $NbZr/NbO_x/Al$ junction, the dependence of voltage at point 11 $V_{quasigap}$ on the temperature (see Fig. 4). Also shown in this figure, for comparison, is the dependence of the voltage at point 2 or V_{gap} on the temperature.

We see that at $T = 4.2$ K the Al has a proximity-effect-induced energy gap of about 1.2 meV, so the proximity effect is large enough through the NbZr/Al interface. In the first case the same current (NbZr is in the resistive, i.e. nonsuperconducting state) cannot produce the measured voltage on the NbO_x barrier, but in the second case (NbZr is in superconducting state) it can produce the measured voltage on the NbO_x barrier; at this applied voltage the behavior of the $NbZr/NbO_x/Al$ junction is similar to that of the SIS tunnel junction.

We assume that this result can be interpreted on the basis of the model [2] for coherent charge transport in superconducting/normal proximity structures, at least qualitatively. We also assume that our experiment demonstrates the presence of a soft (no sharp edge) pseudo gap in the density of states for Al, as shown in model [2].

We have measured the complex junctions with nonuniform order parameter Δ in the electrodes to

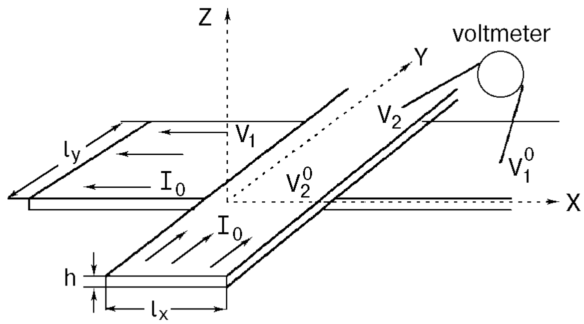

Fig. 5. Measured tunnel junction scheme.

estimate the possibility of the influence of the electrode resistive (nonsuperconducting) state on the junction I–V curves. The junction geometry is shown in Fig. 5. The voltmeter measures the voltage ($V_2 - V_1^0$). But potentials V_1 and V_2 could be functions of the coordinate x and y just as $V_1(x, y)$ and $V_2(x, y)$. We can describe the junction I–V curve as follows:

$$I = f_1 (V_2 - V_1) , \tag{1}$$

$$\text{or } V_2 - V_1 = f_1^+(I) . \tag{2}$$

If the voltage ($V_2 - V_1$) is applied, then the current I flows through the tunnel junction with unit square. We can describe the electrode I–V curve as follows:

$$I = f_2 (V_{22} - V_{21}) ; \tag{3}$$

$$\text{or } V_{22} - V_{21} = f_2^+(I) . \tag{4}$$

If the voltage ($V_{22} - V_{21}$) is applied per unit length of the electrode film, then the current I flows through the electrode film with unit square of cross section (V_{22} and V_{21} are the potentials at point 2 and point 1 of the film 2, respectively). We can express the current through the tunnel junction at the point with the coordinates (x, y) as follows:

$$dI = f_1(V_2 - V_1)\, dx dy, \tag{5}$$

$$I_0 = \int dI = \int_0^{l_x}\int_0^{l_y} f_1 (V_2 - V_1)\, dx dy. \tag{6}$$

Let us consider an imaginary strip (with the coordinate x) which is parallel to the Y axis. We can estimate the potential V_2 distribution in this strip. Because we use a current source for measurements, the current and voltage at the beginning of the strip are

$$I = \frac{I_0}{h l_x} h dx = \frac{I_0}{l_x} dx; \tag{7}$$

$$dV_2 = V_2^0 - V_{21} = f_2^+\left(\frac{I_0}{l_x h}\right) dy. \tag{8}$$

We then have

$$I = \frac{I_0}{l_x} dx - I_{\text{junc}}; \tag{9}$$

$$I_{\text{junc}} = \int_0^y f_1(V_2 - V_1)\, dy\, dx; \tag{10}$$

$$V_2 - V_2^0 = \int_0^y f_2^+\left[\frac{I_0}{l_x h} - \frac{1}{h}\int_0^y f_1 (V_2 - V_1) dy\right] dy. \tag{11}$$

We also have

$$V_1 - V_{1 l_x} = \int_{l_x}^{x} f_2^+\left[\frac{1}{h}\int_{l_x}^{x} f_1(V_2 - V_1)\, dx\right] dx. \tag{12}$$

We can use the equivalent equations for (11), (12)

$$\begin{cases} \dfrac{\partial V_1}{\partial y} = f_2^+\left[\dfrac{1}{h}\displaystyle\int_0^y f_1 (V_2 - V_1)\, dy\right]; \\ \dfrac{\partial V_1}{\partial x} = f_2^+\left[\dfrac{1}{h}\displaystyle\int_{l_x}^x f_1 (V_2 - V_1)\, dx\right]; \\ \dfrac{\partial V_2}{\partial y} = f_2^+\left[\dfrac{I_0}{l_x h} - \dfrac{1}{h}\displaystyle\int_0^y f_1 (V_2 - V_1)\, dy\right]; \\ \dfrac{\partial V_2}{\partial x} = f_2^+\left[\dfrac{I_0}{l_x h} - \dfrac{1}{h}\displaystyle\int_{l_x}^x f_1 (V_2 - V_1)\, dx\right]. \end{cases} \tag{13}$$

We use the function f_2^+ as follows:

$$\begin{cases} V_{22} - V_{21} = 0\,, & \text{if } I \le \dfrac{I_c}{l_x h}\,; \\ V_{22} - V_{21} = b\left(I - \dfrac{I_c}{l_x h}\right), & \text{if } I > \dfrac{I_c}{l_x h}\,. \end{cases} \quad (14)$$

Then

$$\begin{cases} \dfrac{1}{b}\dfrac{\partial^2 V_2}{\partial y^2} = -\dfrac{1}{h} f_1\,(V_2 - V_1)\,; \\ \dfrac{1}{b}\dfrac{\partial^2 V_2}{\partial x^2} = -\dfrac{1}{h} f_1\,(V_2 - V_1)\,; \\ \dfrac{1}{b}\dfrac{\partial^2 V_1}{\partial y^2} = \dfrac{1}{h} f_1\,(V_2 - V_1)\,; \\ \dfrac{1}{b}\dfrac{\partial^2 V_1}{\partial x^2} = \dfrac{1}{h} f_1\,(V_2 - V_1)\,. \end{cases} \quad (15)$$

Here b is the differential resistance of the strip in the resistive (nonsuperconducting) state.

Since we used a current source in the measurement, we have a standard wave equation with initial conditions:

$$\frac{\partial^2 V_2}{\partial x^2} - \frac{\partial^2 V_2}{\partial y^2} = 0\,; \quad (16)$$

$$V_2(x,\,0) = V_2^0\,; \quad (17)$$

$$\left.\frac{\partial V_2}{\partial y}\right|_{y=0} = \frac{bI_0}{l_x h} - \frac{bI_c}{l_x h}\,. \quad (18)$$

So we can used the Dalamber decision of the one-dimentional wave equation in partial derivatives [7]:

$$\begin{aligned} &V_2 - V_1^0 = V_2^0 - V_1^0\,, \quad \text{if } I \le \frac{I_c}{l_x h}\,; \\ &V_2 - V_1^0 = V_2^0 + \frac{b\,(I_0 - I_c)l_y}{l_x h} - V_1^0\,, \quad \text{if } I > \frac{I_c}{l_x h}\,. \end{aligned} \quad (19)$$

In the experiment described above we have not observed this kind of additional voltage as in formula (19). At 12.1 K and 13.0 K we found that the superconducting state of the electrodes does not exist (using the I–V curve of the tunnel junction with AlO_y barrier) and we have the I–V curve for the double junction in this case (see Fig. 3). It is clear that the additional voltage caused by the resistive state in part of the electrode of the investigated junctions can have only a small value as in the I–V curves (Fig. 3), and that the observed additional voltage on the $NbZr/NbO_x/Al$ junction cannot be attributed to this factor.

4. Conclusion

We have prepared and experimentally investigated the tunneling structure $NbZr/NbO_x/Al/AlO_y/NbZr$ with a transparent barrier in the $NbZr/NbO_x/Al$ junction and Al interlayer 4 to 6-nm-thick. In this structure a proximity effect between NbZr and Al through NbO_x barrier has been observed. The voltage on the NbO_x barrier, was produced, and we have observed a coexistence of the proximity effect and applied voltage on the $NbZr/NbO_x/Al$ junction. We believe that this experiment could be described on the basis of the model for coherent charge transport in superconducting/normal proximity structures [2].

1. F. K. Wilhelm, A. D. Zaikin, and G. Schön, *J. Low Temp. Phys.* **106**, 305 (1997).
2. F. K. Wilhelm, A. D. Zaikin, and A. A. Golubov, *J. Low Temp. Phys.* **106**, 297 (1997).
3. H. J. Köhler, P. Seidel, P. Weber, K. Blüthner, S. Linke, and K. H. Berthel, *Phys. Status. Solidi* **67**, 497 (1981).
4. V. M. Pan, E. M. Rudenko, V. P. Gorishnyak, M. V. Belous, S. A. Kosiychuk, Ph. I. Korzhinsky, and V. E. Shaternik, *Cryogenics* **23**, 258 (1983).
5. A. A. Golubov, V. M. Krasnov, and M. Yu. Kupriyanov, *J. Low Temp. Phys.* **106**, 249 (1997).
6. N. Thyssen, A. V. Ustinov, and H. Köhlstedt, *J. Low Temp. Phys.* **106**, 201 (1997).
7. G. A. Korn and T. M. Korn, *Mathematical Haudbook for Scientists and Engineers*, McGrow-Hill Book Company (1968), p. 831.